JOURNAL OF VIROLOGY, May 1991, p. 2640–2646
0022-538X/91/052640-07$02.00/0

Vol. 65, No. 5

Mutations in the Regions of the Rous Sarcoma Virus 3′ Splice Sites: Implications for Regulation of Alternative Splicing

STANTON L. BERBERICH[1]† AND C. MARTIN STOLTZFUS[2]*

Genetics Program[1] and Department of Microbiology,[2] University of Iowa, Iowa City, Iowa 52242

Received 26 October 1990/Accepted 13 February 1991

Retrovirus RNA is synthesized as a single primary transcript that is differentially processed by RNA splicing. Three species of viral RNA (spliced *env*, spliced *src*, and unspliced full-length RNA) are produced in chicken embryo fibroblasts infected with Rous sarcoma virus, an avian retrovirus. The *env* and *src* mRNAs are synthesized by the alternative use of two 3′ splice sites. The mechanism by which balanced splicing at the two sites is maintained was investigated in this report. Mutants that increase or decrease splicing at one of the two 3′ splice sites were analyzed for the effect on splicing at the other site. The two splice sites differed in their response. Mutations that caused a specific increase in the level of spliced *env* mRNA were associated with reciprocal changes in the levels of *src* mRNA but with no change in overall splicing. In contrast, mutants in which the *src* 3′ splice site was inactivated demonstrated a decreased overall level of spliced RNA but had little or no effect on the level of spliced *env* mRNA. Mutations that caused specific increases in the level of spliced *src* mRNA had variable effects on *env* mRNA levels. Deletion of regions in *gag*, which was previously shown to contain a *cis*-acting negative regulator of splicing, resulted in a corresponding increase of both spliced viral mRNAs and a decrease in unspliced RNA, suggesting that this element suppressed both *env* and *src* splicing. Several models are discussed which are possible mechanisms for regulation of alternative splicing of Rous sarcoma virus RNA, but none of these models appear to be consistent with all of the data.

Splicing of retrovirus RNA differs from that of most RNA polymerase II-transcribed host cellular genes, whose primary transcripts are completely spliced before transport to the cytoplasm (19, 22). Retroviruses require the expression of unspliced RNA in the cytoplasm. Therefore, the splicing and transport machinery of the host cell must be manipulated to permit the accumulation of unspliced retrovirus RNA in the cytoplasm (for a review, see reference 25). Retroviruses such as human immunodeficiency virus and human T-cell leukemia virus require virus-encoded functions (*rev* and *rex*, respectively) for the accumulation of unspliced RNA (8, 11, 16, 23). However, most retroviruses apparently do not require these virus-encoded functions (3, 12, 14, 26).

Rous sarcoma virus (RSV), an avian retrovirus, provides an excellent system for studying regulated RNA splicing. The productive infection of RSV in permissive chicken embryo fibroblasts (CEF) requires the expression of three major RNA species from a single precursor RNA that is differentially processed by RNA splicing. The primary transcript contains one major 5′ splice site (5′ss) at nucleotide (nt) 398 (10). The splice is 18 nt downstream from the major AUG used to initiate translation of the *gag*, *pol*, and *env* genes. Two major 3′ splice sites (3′ss) at nt 5078 and 7054 are alternatively spliced to the single 5′ss to form the *env* and *src* mRNAs, respectively (6, 9, 29). The *env* 3′ss is derived from the avian leukosis virus progenitor of RSV, whereas the sequence beginning 17 nt 5′ of the *src* 3′ss is derived from the cellular c-*src* homolog (29).

Several *cis*-acting regions of the RSV genome important in the regulation of levels of spliced and unspliced viral RNA have been identified (3, 13, 26, 27). First, a region in the *gag* gene mapping between nt 708 and 987 (negative regulatory sequence [NRS]) acts in *cis* to suppress splicing in vivo of viral RNA (3, 26). Second, a dramatic increase in the extent of splicing was effected by a specific 24-bp insertion immediately upstream of the *env* 3′ss (13, 14). Although the extent of splicing at *src* was not determined in these experiments, it appeared that most of the increased splicing occurred at the *env* 3′ss and was associated with a virus replication defect. In vitro splicing experiments have indicated that the insertion mutant acts directly on splicing and is associated with the use of a new branchpoint within the inserted sequences (9a). Third, differences in the relative levels of spliced *src* mRNA in cells infected with several different RSV strains were reported. The overspliced phenotype mapped to the noncoding region between *src* and *env*, immediately upstream and downstream of the *src* 3′ss (27).

Although the studies described above have defined *cis*-acting regions which may be important in the regulation of RSV splicing, the effects of the mutations on alternative splicing of *env* and *src* mRNA have not been investigated. In this report, we have measured the extent of splicing at each of the major splice sites of RSV RNA (the 5′ donor, the *env* 3′ acceptor, and the *src* 3′ acceptor) and have determined the effect of mutations at one splice site on the use of the other wild-type splice site. Our results indicate that there are indeed such global effects but that the two 3′ss differ in their response.

MATERIALS AND METHODS

Plasmids. An infectious nonpermuted proviral clone of the RSV Prague A strain contained in pBR322 was obtained from J. Thomas Parsons, University of Virginia, Charlottesville. Infectious plasmid pJTM14 was constructed by cloning the entire provirus derived from pJD100 into a pUC18-based vector. Splicing of viral transcripts derived from pJTM14 was identical to splicing from pJD100 (18a). Deletion mutants were constructed by standard recombinant DNA techniques (17). Plasmids pJDdelBcII (deleted from nt 1149 to

* Corresponding author.
† Present address: Hygienic Laboratory, University of Iowa, Iowa City, IA 52241.

1659) and pJDdelSacII (deleted from nt 544 to 1806) have been described previously (26). Plasmid pJDdelKS was constructed by digesting pJD100 with *Kpn*I and *Sac*II to completion, blunt ending with T4 polymerase, and ligating. This resulted in a deletion in pJD100 from nt 544 to 4995 (nucleotide numbering according to reference 21). Plasmids pSLB-Sac(−23), pSLB-Sac(−79), and pSLB-Sac(−143) are unidirectional BAL 31 deletion clones of pJD100 shown in Fig. 5. These deletions were made in the noncoding region between the *env* gene and the *src* gene starting at the *Sac*I site at nt 6865 and progressing 3′ toward the *src* 3′ss. Deletion endpoints were determined by sequencing according to the method of Sanger et al. (20). Plasmid pJDdelKN was constructed by partial digestion of pJD100 with *Nhe*I and complete digestion with *Kpn*I. The ends were blunt ended with T4 polymerase and ligated, resulting in deletion between nt 4995 and 5131. Plasmid pMPM13 was constructed by removal of the four-base 3′ overhangs of the *Pst*I site at nt 7048 and blunt-end ligation. An additional small deletion within the *src* exon region was created during the construction of pMPM13. Plasmids pMPM7, pMPM8, and pMPM9 (Fig. 1) were constructed by placing fragments from mutated M13 subclones (kindly provided by Duane Grandgenett, St. Louis University Medical Center, St. Louis, Mo.) into pJTM14. Plasmid pMap47 (Fig. 2) was used as a template for RNase mapping. Its construction is described in detail elsewhere (4a).

Cell culture, DNA transfections, and RSV infections. Secondary CEF isolated from embryonated eggs that were negative for both group-specific antigen and chicken helper factor (from SPAFAS Inc., Norwich, Conn.) were grown in SGM (medium 199 [GIBCO BRL] supplemented with 10% [vol/vol] tryptose phosphate broth and 5% calf serum).

CEF were transfected by the DEAE-dextran technique essentially as described by Sompayrac and Danna (24). Purified plasmid DNA (15 μg) in 6 ml of serum-free SGM–0.05 M Tris-HCl (pH 7.4) was used to transfect subconfluent cultures of CEF in 100-mm petri dishes in the presence of 200 μg of DEAE-dextran per ml. After 30 min at room temperature, 2 ml of the transfection mix was removed and 10 ml of serum-free SGM was added. The transfected cultures were incubated at 37°C for 3 h, overlaid with 10 ml of SGM, and incubated at 37°C.

RNA isolation and analysis. Whole cell RNA was isolated from transfected or infected cells by the guanidine hydrochloride technique essentially as described by Strohman et al. (28). The RNA was precipitated with 2.5 volumes 95% ethanol and stored at −20°C.

RNase protection analysis of the RNA samples was carried out essentially as described by Melton et al. (18) as modified by Berberich and Stoltzfus (4a) to optimize conditions of hybridization and digestion for the tandem riboprobe. ^{32}P-labeled probes generated by SP6 polymerase reaction (6×10^6 cpm per sample) were added to appropriate volumes of ethanol-precipitated whole cell RNA (2.5 to 20 μg). The samples were centrifuged, the pellets were washed with 70% ethanol, and the RNA samples were dissolved in 80% formamide–40 mM piperazine-*N*,*N*′-bis (2-ethanesulfonic acid) (PIPES; pH 6.5)–400 mM NaCl–1 mM EDTA. The samples were heated at 85°C for 10 min, hybridized at 60°C for 12 to 16 h, and digested with RNase A (6 μg/ml) and RNase T_1 (300 U/ml) for 30 min at room temperature. Samples were treated and analyzed on 6% polyacrylamide gels containing 7 M urea as described elsewhere (4a). After electrophoresis, the gel was dried and exposed to X-ray film. The autoradiograms were scanned, and the resulting integrated values for the appropriate bands on the gel were corrected for relative nucleotide composition, using the values obtained for the Prague C RSV sequence (21). The levels of viral RNA were corrected for the contribution of c-*src* in the spliced *src* band. Because of mismatches between the c-*src* and v-*src* sequences, RNase digestion of the hybrids resulted in the generation of a characteristic lower-molecular-weight band from c-*src* (marked with an asterisk in Fig. 3) in addition to a residual band at the position of spliced v-*src*. To correct the amounts of radioactivity in the v-*src* band for the contribution of c-*src*, the ratio of the upper and lower bands was determined in the mock-transfected negative control lane. This ratio varied with the conditions of RNase digestion but was consistent within a single experiment. The value could then be used to correct for the c-*src* contribution in the experimental samples.

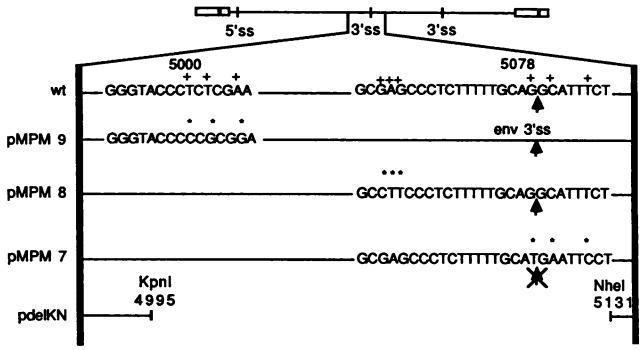

FIG. 1. Schematic representation of *env* 3′ss mutants. Symbols: *, location of mutations; +, site of mutation in the wild-type (wt) genome. The *env* 3′ss is marked by a vertical arrow.

Northern blot analysis of RNA was carried out on formaldehyde-containing agarose gels essentially as described by Maniatis et al. (17).

Materials. Restriction enzymes and other enzymes used for cloning and the analysis of recombinant DNA were purchased from Boehringer Mannheim Biochemicals Co. (Indianapolis, Ind.) and Bethesda Research Laboratories (Gaithersburg, Md.). SP6 polymerase was purchased from Promega Co. (Madison, Wis.). RNase A was purchased from Sigma (St. Louis, Mo.), and RNase T_1 was purchased from Boehringer Mannheim.

RESULTS

Mutations in the region of the *env* splice site affect 3′ss choice but not overall splicing. Several proviral mutants of the Prague A RSV in the region of the *env* 3′ss were used in these studies (Fig. 1). Plasmid pMPM9 has three mutated bases approximately 75 nt upstream of the 3′ss. This clone was noninfectious as a result of a lesion in the integrase gene (9b). Plasmid pMPM8 has three altered bases at 15, 16 and 17 nt upstream from the *env* 3′ss; this results in an increase in the length (from 10 to 14 nt) of the polypyrimidine tract upstream from the *env* 3′ss. This clone was infectious but demonstrated a delayed replication phenotype (9b). Plasmid pMPM7 was mutated at the 3′ss itself; in this mutant, the conserved 3′ AG was changed to AT. This mutation would be expected to completely block *env* splicing (1). As expected for such a mutant, pMPM7 was noninfectious. Finally, plasmid pdelKN was deleted in the region from nt 4995 to 5135, which includes the *env* 3′ss at 5074. This clone was also noninfectious.

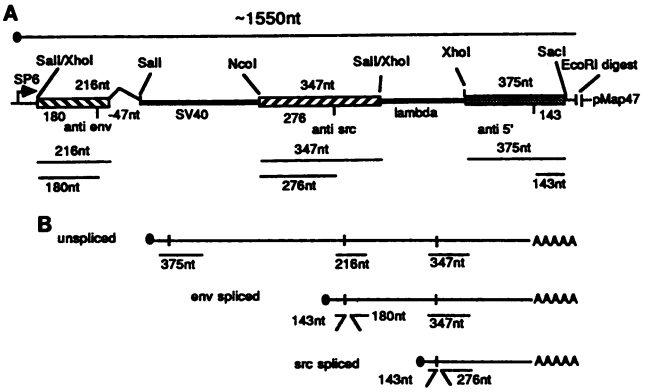

FIG. 2. Products of RNase mapping of viral RNAs, using a riboprobe derived from SP6 transcription of pMap47. (A) Regions contained within the *Eco*RI-digested pMap47 (*env*, ▨; *src*, ▨; 5′, ▩). The SP6 transcript of approximately 1,550 nt is shown above the plasmid map. Below the plasmid map are shown the protected fragments resulting from hybridization to viral RNA followed by RNase digestion. (B) Schematic representation of the protected fragments derived from each of the three major viral mRNAs (unspliced, *env*, and *src*) when hybridized to pMap47 ^{32}P-labeled RNA. Note that the 347-nt unspliced *src* band arises from both unspliced RNA and *env* spliced mRNA.

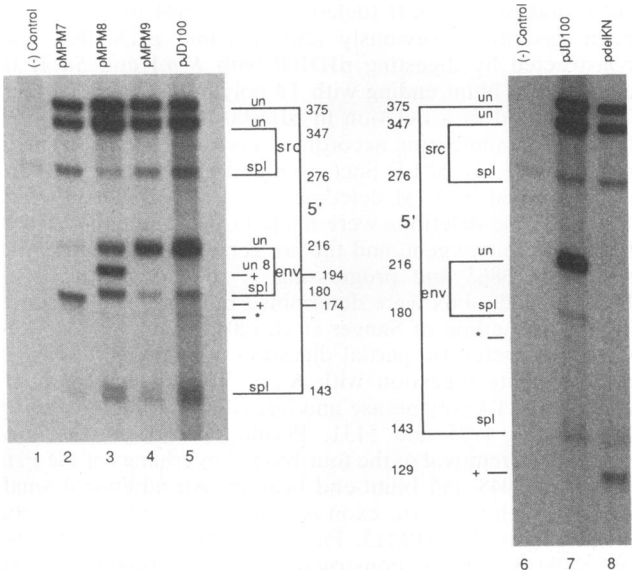

FIG. 3. Effects of mutations in the region of the *env* 3′ss on levels of viral RNA species. Shown is an RNase protection map obtained by using a riboprobe and whole cell RNA (amounts given for each lane) from CEF harvested 48 h after transfection with no DNA (lane 1; 10 μg), pMPM7 (lane 2; 10 μg), pMPM8 (lane 3; 10 μg), pMPM9 (lane 4; 10 μg), pJD100 (lane 5; 10 μg), no DNA (lane 6; 10 μg), pJD100 (lane 7; 5 μg), and pdelKN (lane 8; 10 μg). The bands designated + indicate the altered location of the unspliced *env* band due to the base changes in pMPM8 and pMPM7 and the deletion in pdelKN. Incompletely digested unspliced *env* fragments are also present in pMPM8 and pMPM7 because of the inefficiency of the RNase activity at the mutation sites. The RNase activity is more efficient for pMPM7, in which the base changes disrupt a stretch of seven bases, in contrast to pMPM8, in which only three bases are disrupted. *, Band present in the control RNA that is used to determine the amount of c-*src* present in the samples as described in Materials and Methods. un, Unspliced; spl, spliced.

To analyze splicing of these mutant clones, plasmid DNA was introduced by transfection into CEF and total cellular RNA was isolated after 48 h. To obtain quantitative data on the extents of splicing and the levels of *env* and *src* mRNAs, RNA was analyzed by using a tandem [^{32}P]uridine-labeled antisense riboprobe spanning the major 3′ss and the major 5′ss (4a). The structure of the mapping clone pMap47 is shown in Fig. 2A. Characteristic protected species from each region of the probe were produced after hybridization to the wild-type pJD100 RNA (Fig. 2B).

The results of RNase mapping of RNA from cells transfected by pMPM9, which was mutated in a region 75 nt upstream from the *env* 3′ss, is shown in Fig. 3, lane 4. As shown in Table 1, the relative amounts of the three viral RNA species were not significantly different from the values for the wild-type pJD100, whose map is shown in Fig. 3, lane 5. This finding indicates that the base changes in pMPM9 have no apparent effect on splicing. This is not surprising, since the mutations are relatively far from the *env* 3′ss. These data also establish that the values obtained for the noninfectious clone pMPM9, which is not capable of virus spread, are not significantly different from those of the infectious wild-type clone pJD100. The result of RNase mapping of RNA from cells transfected with pMPM8, which has a polypyrimidine tract longer than that of the wild type, is shown in Fig. 3, lane 3. Because of the mismatch between the probe and the mutant RNA at the site of the mutation, the hybrids were cleaved with RNase at the site of the mismatch. This resulted in the production of a smaller unspliced *env* band (~200 nt; un 8$^+$ in Fig. 3). A band also migrated at the position of normal *env* unspliced RNA-protected fragment. This band reflected incomplete RNase digestion at the site of mismatch and was included in calculating the total for unspliced *env* RNA. An increase in the relative molar amount of spliced *env* mRNA from 13 to 26% and a decrease in amount of spliced *src* mRNA from 12 to 3% was observed in cells transfected with pMPM8 (Table 1). However, the overall ratio of unspliced to spliced RNA (*env* plus *src*) was not significantly different from the wild-type value. This was confirmed by quantitative analysis of the relative amounts of the unspliced and spliced bands derived from the 5′ region of the probe (71 and 31%, respectively).

RNase mapping of RNA from cells transfected with the *env* 3′ss mutant pMPM7 indicated that a fragment migrating more rapidly than the normal spliced 180-nt *env* protected fragment (marked +) was protected (Fig. 3, lane 2). This band was derived by cleavage of the probe hybridized to unspliced RNA derived from pMPM7 at the positions of the mutations as shown in Fig. 1. A minor band migrating at the position of the normal unspliced *env* fragment was also present (as with RNA from pMPM8-transfected cells) and resulted from incomplete RNase cleavage of the probe at the mismatched bases of the hybrids. The relative amount of spliced *src* mRNA in pMPM7-transfected cells (determined from the ratio of unspliced *src* to spliced *src*) was increased from 12 to 28%, but the overall level of spliced RNA was not significantly different from the wild-type value (25 versus 28%) (Table 1). This result was confirmed by quantitative analysis of the relative amounts of unspliced and spliced bands derived from the 5′ region of the probe (73 and 27%, respectively).

To confirm that the removal of the *env* 3′ss did not significantly affect the overall level of splicing, we analyzed RNA in cells transfected by plasmid pdelKN, in which the

TABLE 1. Relative molar amounts of viral RNA species in CEF transfected with proviral DNA mutated within the *env* splice site region[a]

RNA	% of RNA molecules				
	pJD100 (wt) (n = 6)	pMPM9 (n = 6)	pMPM8 (n = 2)	pMPM7 (n = 5)	pdelKN RNA (n = 2)
Unspliced	74.7 (5.0)	74.0 (3.5)	71.5 (5.0)	72.1 (3.5)	73.5 (3.5)
src	12.3 (2.6)	13.1 (2.4)	3.0 (1.4)	27.9 (3.5)	26.5 (3.5)
env	13.1 (2.7)	13.0 (1.7)	25.5 (6.4)		

[a] The intensities of the bands were determined by densitometry and corrected for the number of uridine residues in the protected band, and the contributions of c-*src* were subtracted from the spliced *src* band as described in Materials and Methods. The 276-nt spliced *src* band was used for total *src* mRNA, the 180-nt spliced *env* band was used for total *env* mRNA, and the unspliced *env* band (whose size varies with the particular mutant clone; see Fig. 1) was used for total unspliced mRNA. In the case of pMPM7 and pdelKN, the 347-nt unspliced *src* band was used to quantitate total unspliced mRNA. The ratios of the 375-nt unspliced 5′ band and 143-nt spliced 5′ band were also determined, and these values were similar in each case to the ratios of unspliced/(*env* + *src*). The determined value for each of these bands was individually divided by the sum total of the three bands and multiplied by 100 to give percent RNA. n, Number of independent determinations. Standard deviations are given in parentheses. wt, Wild type.

env splice site region was deleted (Fig. 3A, lane 8). An increase in the relative amount of *src* mRNA was observed (from 12 to 27%), but as observed for the *env* splice site mutant pMPM7, the level of total spliced RNA did not change significantly (Table 1). Thus, each of the mutations that we studied in the region of the *env* 3′ss resulted in changes in the relative levels of spliced *env* and *src* mRNAs but did not change the overall extent of splicing.

Confirmatory evidence for the types of viral mRNA species in cells transfected with the *env* 3′ss mutant pMPM7 was obtained by Northern blot analysis using a probe derived from the long terminal repeat and 5′ *gag* region which hybridizes to all viral RNA species (Fig. 4). The small amounts of viral RNA which are present in transfected cells necessitated relatively long exposures of the autoradiogram with concomitant background hybridization. For this reason, two exposures of the Northern blot are shown. At 24 h of exposure (Fig. 4A), an *env* mRNA band was detected in the pJD100 lane but not in the pMPM7 lane. A faint band migrating at the position of the *env* mRNA was detected in the pMPM7 lane at 72 h of exposure. This band migrated more rapidly than *env* mRNA when longer times of electrophoresis were carried out, and it corresponds to a *src* mRNA 3′ readthrough product (18a). The RNA signal from pMPM7 was lower than that from pJD100, probably because the wild-type pJD100 clone is infectious and the signal is increased as a result of some spread of infectious virus during the 48-h transfection. Since pMPM7 is noninfectious, it cannot spread as virus. The results of the Northern blot indicated that the *env* mRNA band from pJD100 was less intense than the *src* mRNA band, whereas the RNase protection data (Table 1) showed that there were comparable amounts of both mRNAs. We have found that the RNase protection data were more reliable than Northern blots and attribute the difference in results to inefficient binding of *env* mRNA to the membrane in the Northern blot. This may result from competition for binding to the membrane from the 28S rRNA which migrates just ahead of the *env* mRNA.

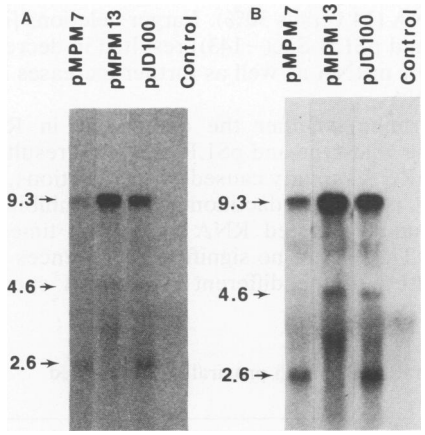

FIG. 4. Northern blot analysis of 3′ss mutants. RNA samples (10 μg) from cells transfected with *env* 3′ss mutant pMPM7, *src* 3′ss mutant pMPM13, wild-type pJD100, and no-DNA control were electrophoresed on formaldehyde-agarose gels and blotted onto nylon membranes. Hybridization was carried out for 16 h with a ^{32}P-labeled riboprobe complementary to the 5′ 630 nt and 3′ ~300 nt of the genomic RNA. Two exposures of the autoradiogram are shown (A, 24 h; B, 72 h).

Mutations in the region of the *src* splice site affect overall splicing but have less effect on *env* splicing. To determine the effect of inactivating the *src* 3′ss, viral RNA from cells transfected with a proviral clone (pMPM13) with a 4-bp deletion at the *src* 3′ss was studied. Northern blot analysis of the RNA shown in Fig. 4 indicated the expected absence of a *src* mRNA band. The smear of radioactivity migrating between the *env* and *src* bands was apparent in the longer exposure (Fig. 4B) and was also present in the wild-type RNA control. This may arise from partially degraded RNA in the samples. The result of RNase protection mapping of MPM13 is shown in Fig. 5, lane 1. A number of bands were derived by hybridization of unspliced RNA from pMPM13 to the *src* probe (mutant *src* bands). The band migrating at the position of the normal spliced *src* protected fragment (276 nt) resulted from incomplete RNase digestion at the mismatch between the hybrid and the probe. The extent of splicing at the *env* 3′ss was calculated from the ratio of unspliced and spliced *env* protected fragments (Table 2). An increase in the relative amount of unspliced RNA in cells transfected with pMPM13 was observed (86 versus 72% in wild-type pJD100), but no significant change occurred in the level of spliced *env* mRNA (14 versus 13%). The results based on the 5′ region of the probe were also in good agreement with this result (84% unspliced; 16% spliced).

Previous results suggested that differences in the noncoding region between the *env* and *src* genes were responsible for different extents of splicing at the *src* 3′ss in two strains of RSV (27). To further study the effect of this region on splicing, a series of unidirectional 3′ deletions (Fig. 6) were made in pJD100 from the *Sac*I site at nt 6865 3′ toward the *src* splice site at nt 7054. Cells transfected with cloned

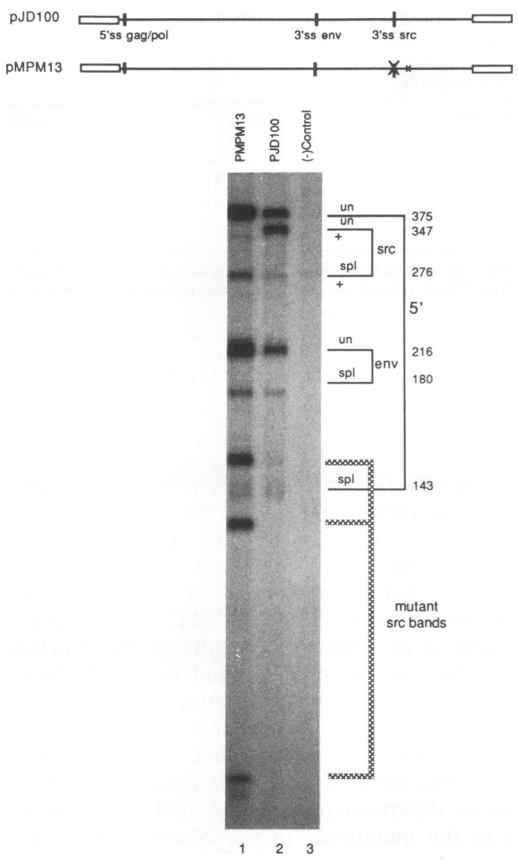

FIG. 5. Effects of inactivating the *src* 3'ss on levels of viral RNA species. Shown is an RNase protection map obtained by using a ^{32}P-labeled riboprobe transcribed from pMPM47 and whole cell RNA (amounts given for each lane) from CEF harvested 48 h after transfection with pMPM13 (lane 1; 10 μg), pJD100 (lane 2; 5 μg), and no DNA (lane 3; 10 μg). The identities and locations of these various protected bands are indicated. The smaller *src*-specific bands arising from unspliced RNA in pMPM13 transfected cells are indicated. +, Incompletely digested bands. un, Unspliced; spl, spliced.

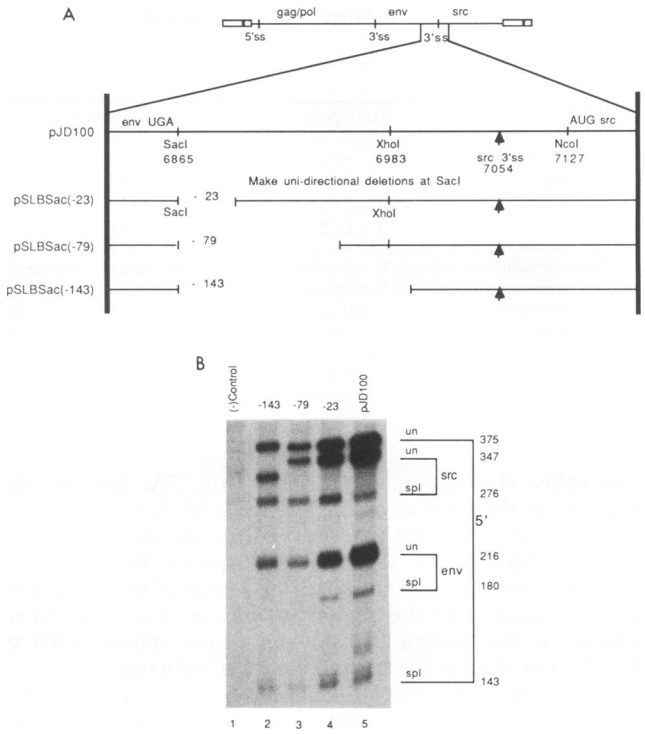

FIG. 6. Effects of deletions in the noncoding region between *env* and *src* on levels of viral RNA species. (A) Schematic representation of the various-size unidirectional deletions made in pJD100. (B) RNase protection map obtained by using a ^{32}P-labeled riboprobe transcribed from pMap47 and whole cell RNA (5 μg) from CEF transfected 48 h earlier with the indicated plasmids. The unspliced *src* band at pSLB Sac(−143) migrated more rapidly than the equivalent pJD100 band because the 3′ endpoint of the deletion is 28 bp downstream of the *Xho*I site, the 3′ endpoint of the antisense probe (see Fig. 2). Thus, a smaller protected unspliced *src* fragment was produced. un, Unspliced; spl, spliced.

proviral DNA (Fig. 6) were analyzed by RNA protection assays and were compared with wild-type controls. The results indicated that the relative levels of spliced *src* mRNA were increased whereas the relative amounts of unspliced RNA were correspondingly decreased. The increase in the extent of splicing was confirmed in each case by determining the ratio of the 5′ unspliced to 5′ spliced bands (data not shown). In cells transfected with the smallest deletion mutant [pSLB-Sac(−23)], the level of spliced *env* mRNA was not significantly different from the wild-type value even though there was greater than a twofold increase in the level of *src* mRNA (14 versus 30%). Larger deletions [i.e., pSLB-Sac(−79) and pSLB-Sac(−143)] resulted in decreases in the levels of *env* mRNA as well as further increases in the level of *src* mRNA.

To determine whether the differences in RNA levels between the wild-type and pSLB-Sac(−23) resulted from an effect on mRNA stability caused by the deletions, we treated transfected cells with dactinomycin, an inhibitor of transcription, and harvested RNA at various times after the treatment. There were no significant differences in the relative stabilities of the different viral RNA species in the

TABLE 2. Relative molar amounts of viral RNA species in CEF transfected with proviral DNA mutated within the *src* splice site region[a]

RNA	% of RNA molecules				
	pJD100 (wt) (n = 3)	pMPM13 (n = 7)	pSLB(−23) (n = 3)	pSLB(−79) (n = 3)	pSLB(−143) (n = 3)
Unspliced	72.4 (3.6)	85.8 (1.9)	59.7 (2.9)	54.2 (0.9)	55.3 (1.9)
src	14.3 (0.9)		30.1 (2.2)	40.5 (0.8)	38.0 (1.1)
env	13.2 (2.8)	14.2 (2.0)	10.2 (0.8)	5.3 (1.2)	6.5 (1.2)

[a] Calculations were carried out as for Table 1. n, Number of independent determinations. Standard deviations are given in parentheses. wt, Wild type.

TABLE 3. Relative molar amounts of viral RNA species in CEF transfected with proviral DNA deleted in *gag* and *pol*[a]

RNA	% of RNA molecules			
	pJD100 (wt) (n = 10)	pdelBclI (Δ1149-1659) (n = 3)	pdelSacII (Δ544-1806) (n = 3)	pdelKS (Δ544-4995) (n = 4)
Unspliced	74.1 (4.0)	73.6 (2.7)	47.1 (4.3)	32.8 (7.1)
src	13.0 (2.6)	11.6 (2.2)	27.1 (3.5)	34.2 (2.9)
env	12.8 (2.3)	14.8 (1.7)	25.8 (1.1)	33.0 (4.3)

[a] Calculations were carried out as for Table 1. n, Number of independent determinations. Standard deviations are given in parentheses. The location of the deletion in the viral genome (Δ) is indicated by nucleotide number. wt, Wild type.

wild-type- and mutant-transfected cells (data not shown). Therefore, the differences in relative RNA levels exhibited by this mutant likely result from splicing rather than from differential RNA stabilities.

Deletions in *gag* and *pol* do not affect splice site usage. A negative *cis*-acting sequence (NRS) in the *gag* gene acts to increase the accumulation of unspliced RNA in vivo, presumably by inhibiting splicing (3, 26). To determine whether deletion of this region affects the relative distribution of spliced *src* and *env* mRNAs, we used the tandem riboprobe described above. A clone with a *gag* deletion but containing the NRS region of *gag* (pdelBclI) showed the same overall extent of splicing and *env*-to-*src* ratios as the wild type, pJD100 (Table 3). A clone with a *gag* deletion which included the *gag* NRS region (pdelSacII) and a clone with both an NRS and *env* intron deletion (pdelKS) demonstrated increases in the relative levels of spliced RNA (47 and 67% spliced, respectively, versus 30% spliced in the wild-type pJD100-transfected cells) (Table 3). The relative increase in levels of spliced RNA species is not due to decreased stability of unspliced RNA with the NRS deletion (3; 18a). The molar ratios of *env* to *src* mRNAs in both pdelSacII- and pdelKS-transfected cells were similar to the wild-type value (approximately 1:1) (Table 3). These results indicated that even though the level of spliced viral RNA was significantly increased in cells transfected with pdelSacII and pdelKS, the ratio of spliced *env* and *src* mRNA levels was not significantly altered. This result suggests that the regions of the genome affecting the balance of *src* and *env* mRNAs lie outside the deleted regions, i.e., outside the region deleted in pdelKS (nt 543 to 4995).

DISCUSSION

We have shown in this report that mutants in which the *env* and *src* 3'ss were inactivated appear to have different effects on splicing at the corresponding unmutated 3'ss (Tables 1 and 2). A mutant at the *env* 3'ss in which *env* splicing was prevented (pMPM7) was associated with a concomitant increase in the level of spliced *src* mRNA. Similar results were obtained with a mutant in which the *env* 3'ss region was deleted (pdelKN). In contrast, the level of spliced *env* mRNA was not significantly affected when the *src* splice site was inactivated. In light of these results, we have considered three models to explain alternative use of RSV RNA 3'ss. (i) Splicing at the *env* and *src* 3'ss is determined by competition between the two respective 3'ss for the major 5'ss. This model does not explain why mutation of the *src* 3'ss does not significantly affect the extent of splicing at the *env* 3'ss (Table 2). (ii) Two separate nuclear pools of RNA precursors are used for splicing at the *env* and *src* 3'ss. This model does not explain how mutations near the *env* 3'ss can have reciprocal effects on splicing at the *src* 3'ss (Table 1). (iii) Commitment to splicing at the *env* 3'ss and *src* 3'ss (but not necessarily the execution of splicing) is cotranscriptional, and formation of spliceosomes at the *env* 3'ss can occur only for a brief time following synthesis of the *env* 3'ss. This model is consistent with data from other laboratories suggesting that in vivo, spliceosome formation may occur during transcription on nascent RNA chains (1, 2, 5, 7, 15). It is also consistent with data that mutations affecting the *env* 3'ss have a reciprocal effect on splicing at the *src* 3'ss but that inactivation of the *src* 3'ss does not change the level of spliced *env* mRNA.

The results with a mutant in which a selective increase in levels of spliced *env* mRNA occurred (pMPM8) also were consistent with the cotranscriptional model, since the increase in *env* mRNA was concomitant with a reciprocal decrease in *src* mRNA. The mechanism by which this mutation may increase splicing at the *env* 3'ss is not yet clear. The sequence upstream of the 3'ss of metazoan precursor RNAs includes a branchpoint sequence at a distance of 10 to 40 nt from the 3'ss (consensus sequence is YNYURAY; the branchpoint is underlined), a polypyrimidine tract, and an AG dinucleotide (14a). The importance of the polypyrimidine tract in RNA splicing has previously been shown (4, 30, 31), and thus the increased length of this element in the RNA of pMPM8 may allow for more efficient splicing at the *env* splice site. Alternatively, the branchpoint in this mutant may be different from the wild-type site, since a potential branchpoint consensus sequence GCGAG (the branchpoint is underlined) is changed to GCCUU, which is not a consensus branchpoint sequence. Indeed, in vitro splicing experiments in HeLa cell nuclear extracts have shown that the wild-type sequence serves as a weak branchpoint for splicing at the RSV *env* 3'ss (9a). Fu et al. (9a) also showed that use of alternative branchpoints in some mutants could be correlated with changes in splicing in vitro.

The results of our studies of mutants in which the levels of spliced *src* mRNA were selectively increased did not fit any of the three models proposed above. We have shown that deletion mutations in the region between *env* and *src* selectively increased the level of *src* mRNA and decreased the level of unspliced RNA (Table 3). These mutations were associated with variable effects on the levels of spliced *env* mRNA. The smallest deletion (23 nt) had no significant effect on *env* mRNA levels, whereas larger deletions (79 and 143 nt) were associated with decreases in *env* mRNA levels. The mechanism by which these mutations might cause an increase in splicing at the *src* 3'ss is not clear. The smallest 23-nt deletion does not impinge upon the upstream member of the ~115-bp direct repeat elements flanking the *src* gene; we therefore do not believe that this is the cause of the effect. It is also of interest that the region of the viral genome responsible for differences in splicing at the *src* 3'ss between the Prague A and C RSV strains mapped between the *env* and *src* genes. However, the locations of the four nucleotide differences between the strains in the region between *env* and *src* were outside the 23- and 79-nt deletions (27). This finding suggests that several separate elements in the *env-src* intergenic region may affect splicing at the *src* 3'ss.

Finally, we have shown that neither an intact *src* 3'ss nor *env* 3'ss is required to maintain a pool of unspliced RNA. These observations are consistent with our previous data showing that deletion of 80% of the *src* intron, including the *env* 3'ss, still allowed the accumulation of significant

amounts of unspliced RNA (26). We have also confirmed earlier results indicating that both *env* and *src* are affected to similar extents by *gag* NRS deletions (Table 3; 26). The presence of the NRS element only partially explains the accumulation of unspliced RNA, since mutants in which the entire NRS is deleted still maintain 30 to 50% of their RNA as unspliced RNA. Clearly, a full understanding of how avian sarcoma viruses undergo balanced splicing and maintain approximately equal levels of *env* and *src* mRNAs will require further genetic analyses and correlation with in vitro splicing experiments.

ACKNOWLEDGMENTS

This work was supported by Public Health Service grant CA28051 from the National Cancer Institute. S.L.B. was supported by Public Health Service National Research Service Award GM07091 from the National Institute of General Medical Sciences.

We thank Z. Cai for technical assistance, M. Reeve for typing, and S. Perlman and M. Stinski for critical reading of the manuscript.

REFERENCES

1. **Abei, M., H. Hornig, R. A. Padgett, J. Reiser, and C. Weissman.** 1986. Sequence requirements for splicing of higher eukaryotic nuclear pre-mRNA. Cell **47**:555–565.
2. **Adami, G., and J. R. Nevins.** 1986. Splice site selection dominates over poly(A) site choice in RNA production from complex adenovirus transcription units. EMBO J. **7**:2107–2116.
3. **Arrigo, S., and K. Beemon.** 1988. Regulation of Rous sarcoma virus RNA splicing and stability. Mol. Cell. Biol. **8**:4858–4867.
4. **Beldjord, C., C. Lapoumeroulie, J. Pagnier, M. Benabadji, R. Krishnamoorthy, D. Labie, and A. Bank.** 1988. A novel β thallassemia gene with a single base mutation in the conserved polypyrimidine sequence at the 3′ end of 1VS2. Nucleic Acids Res. **16**:4927–4935.

4a. **Berberich, S. L., and C. M. Stoltzfus.** Analysis of spliced and unspliced Rous sarcoma virus RNAs early and late after infection of chicken embryo fibroblasts: effect of cell culture conditions. Virology, in press.

5. **Beyer, A. L., and Y. N. Osheim.** 1988. Splice site selection, rate of splicing, and alternative splicing on nascent transcripts. Genes Dev. **2**:754–765.
6. **Chang, L.-J., and C. M. Stoltzfus.** 1985. Cloning and nucleotide sequences of cDNAs spanning the splice junctions of Rous sarcoma virus mRNAs. J. Virol. **53**:969–972.
7. **Eperon, L. P., I. R. Graham, A. D. Griffiths, and I. C. Eperon.** 1988. Effects of RNA secondary structure on alternative splicing of pre-mRNA: is folding limited to a region behind the transcribing RNA polymerase? Cell **54**:393–401.
8. **Feinberg, M. B., R. F. Jarett, A. Aldovini, R. C. Gallo, and F. Wong-Staal.** 1986. HTLV-III expression and production involve complex regulation at the levels of splicing and translation of viral RNA. Cell **46**:807–817.
9. **Ficht, T. A., L.-J. Chang, and C. M. Stoltzfus.** 1984. Avian sarcoma virus *gag* and *env* gene structural protein precursors contain a common aminoterminal sequence. Proc. Natl. Acad. Sci. USA **81**:362–366.

9a. **Fu, X.-D., R. Katz, A. M. Skalka, and T. Maniatis.** 1991. The role of branchpoint and 3′ exon sequences in the control of balanced splicing of avian retrovirus RNA. Genes Dev. **5**:211–220.

9b. **Grandgenett, D.** Personal communication.

10. **Hackett, P. B., H. E. Varmus, and J. M. Bishop.** 1981. The genesis of Rous sarcoma virus messenger RNAs. Virology **112**:714–728.
11. **Hidaka, M., J. Inoue, M. Yoshida, and M. Seiki.** 1988. Post-transcriptional regulator (rex) of HTLV-1 initiates expression of viral structural proteins but suppresses expression of regulatory proteins. EMBO J. **7**:519–523.
12. **Hwang, L.-H., J. Park, and E. Gilboa.** 1984. Role of intron-contained sequences in formation of Moloney murine leukemia virus *env* mRNA. Mol. Cell. Biol. **4**:2289–2297.
13. **Katz, R. A., M. Kolter, and A. M. Skalka.** 1988. *cis*-acting intron mutations that affect the efficiency of avian retroviral RNA splicing: implications for mechanisms of control. J. Virol. **62**:2686–2895.
14. **Katz, R. A., and A. M. Skalka.** 1990. Control of retrovirus splicing through maintenance of suboptimal processing signals. Mol. Cell. Biol. **10**:696–704.

14a. **Krainer, A., and T. Maniatis.** 1988. RNA splicing, p. 131–296. *In* B. D. Hames and M. D. Glover (ed.), Frontiers in molecular biology: transcription and splicing. IRL Press, Oxford.

15. **Leff, S. E., R. M. Evans, and M. G. Rosenfeld.** 1987. Splice commitment dictates neuron-specific alternative RNA processing in calcitonin/CGRP gene expression. Cell **48**:517–524.
16. **Malim, M. H., J. Hauber, R. Fenrick, and B. R. Cullen.** 1988. Immunodeficiency virus rev trans-activator modulates the expression of viral regulatory gene. Nature (London) **335**:181–183.
17. **Maniatis, T., E. F. Fritsch, and J. Sambrook.** 1982. Molecular cloning: a laboratory manual. Cold Spring Harbor Laboratory, Cold Spring Harbor, N.Y.
18. **Melton, D. A., P. A. Kreig, M. R. Rebagliati, T. Maniatis, K. Zinn, and M. R. Green.** 1984. Efficient *in vitro* synthesis of biologically active RNA and RNA hybridization probes from plasmids containing a bacteriophage SP6 promoter. Nucleic Acids Res. **12**:7035–7056.

18a. **Miller, J. T., and C. M. Stoltzfus.** Unpublished data.

19. **Padgett, R. A., P. J. Grabowski, M. M. Konarska, S. Seiler, and P. A. Sharp.** 1986. Splicing of messenger RNA precursors. Annu. Rev. Biochem. **55**:1119–1150.
20. **Sanger, F., S. Nicklen, and A. R. Coulson.** 1977. DNA sequencing with chain-terminating inhibitors. Proc. Natl. Acad. Sci. USA **74**:5463–5467.
21. **Schwartz, D. E., R. Tizard, and W. Gilbert.** 1983. Nucleotide sequence of Rous sarcoma virus. Cell **32**:853–869.
22. **Sharp, A. P.** 1987. Splicing of messenger RNA precursors. Science **235**:766–771.
23. **Sodroski, J., W. C. Goh, C. Rosen, A. Dayton, E. Terwilliger, and W. Haseltine.** 1986. A second post-transcriptional trans-activator gene required for HTLV-III replication. Nature (London) **321**:412–417.
24. **Sompayrac, L. M., and K. J. Danna.** 1981. Efficient infection of monkey cells with DNA and SV40. Proc. Natl. Acad. Sci. USA **78**:7575–7578.
25. **Stoltzfus, C. M.** 1988. Synthesis and processing of avian sarcoma retrovirus RNA. Adv. Virus Res. **35**:1–38.
26. **Stoltzfus, C. M., and S. J. Fogarty.** 1989. Multiple regions in the Rous sarcoma virus *src* gene intron act in *cis* to affect the accumulation of unspliced RNA. J. Virol. **63**:1669–1676.
27. **Stoltzfus, C. M., S. K. Lorenzen, and S. L. Berberich.** 1987. Noncoding region between the *env* and *src* genes of Rous sarcoma virus influences splicing efficiency at the *src* gene 3′ splice site. J. Virol. **61**:177–184.
28. **Strohman, R., P. Moss, J. Micou-Eastwood, D. Spector, A. Przybyla, and B. Peterson.** 1977. Messenger RNA for myosin polypeptides: isolation from single myogenic cell cultures. Cell **10**:265–273.
29. **Swanstrom, R., R. C. Parker, H. E. Varmus, and J. M. Bishop.** 1983. Transduction of a cellular oncogene: the genesis of Rous sarcoma virus. Proc. Natl. Acad. Sci. USA **80**:2519–2523.
30. **van Santen, L. V., and R. A. Spritz.** 1985. mRNA precursor splicing in vivo: sequence requirements determined by deletion analysis of an intervening sequence. Proc. Natl. Acad. Sci. USA **82**:2885–2889.
31. **Wieringa, B., E. Hofer, and C. Weissmann.** 1984. A minimal intron length but no specific internal sequence is required for splicing the large rabbit beta-globin intron. Cell **37**:743–751.